



## THERMAL AND OPTICAL STUDIES OF MIXED ALKALI-ALKALINE EARTH OXIDE BORATE GLASSES

G. SRINIVAS, J. SIVA KUMAR, MD. SHAREFUDDIN, M. N CHARY, R. SAYANNA.

Department of physics, Osmania University, Hyderabad, India.

Email: srinu123g@gmail.com

### ABSTRACT

Glasses with the composition  $xK_2O-(25-x)Na_2O-12.5MgO-12.5BaO-50B_2O_3$  ( $x = 0, 5, 10, 15, 20$  and  $25$ mol %) were synthesized by the melt-quenching technique and were characterized using X-ray diffraction technique at room temperature. Physical parameters like density, oxygen packing density, molar volume and glass-transition temperature and optical parameters, like direct, indirect band gap, cut-off wavelength and Urbach energy values were evaluated. These data was used to understand the mixed alkali effect in the glass matrix. Differential scanning calorimeter (DSC) was used to determine the glass-transition temperature ( $T_g$ ). From the optical absorption studies the values of the optical band gap ( $E_{opt}$ ) for indirect transition, optical edge, cut-off wavelength, and Urbach energy ( $\Delta E$ ) have been evaluated. The values of  $E_{opt}$ ,  $\Delta E$ , glass-transition temperature and cut-off wavelength show nonlinear behavior with the  $K_2O$  content which may be due to mixed alkali effect. Density and molar volume also show nonlinear and opposite behavior with the  $K_2O$  content which also may be due to the mixed alkali effect in the present glass system.

**Keywords:** Borate glasses, Differential scanning calorimeter (DSC), Optical absorption spectra, and mixed alkali effect.

### 1. INTRODUCTION:

Mixed alkali borate glasses are particularly interesting model systems as they exhibit a variety of structural changes with alkali content. If one alkali ion gradually replaces the alkali ion keeping total alkali content as constant. it was noticed that many physical properties of oxide glasses have shown non-linear behavior exhibiting a maximum or minimum. This phenomenon is termed as 'Mixed Alkali Effect' (MAE) and is observed for properties associated with alkali ion movement such as electrical conductivity, dielectric relaxation and internal friction [1]. The mixed alkali effect is one of the classic anomalies of glass science [2, 3] and has been the subject of study over the years [4, 5]. The boroxol group is composed of three corner sharing  $BO_3$  triangles, which form a planar ring. It is well known that the addition of alkali or alkaline earth oxides to  $B_2O_3$  changes some  $BO_3$  triangles to  $BO_4$  tetrahedral. Moreover, the alkali [ $M^+$ ] or the alkaline earth [ $M^{2+}$ ] cations act as network modifiers in the glass structure breaking bridging oxygen bonds to form non-bridging oxygens (NBO) [6] and extends their scope of applications. Structural changes above the glass transition temperature ( $T_g$ ) are expected to have drastic consequences on the transport (viscosity, diffusion) and thermodynamic (molar expansivity, compressibility, heat capacity) properties of melts. An adequate understanding of the temperature dependence of melt properties requires information on both structure and dynamics. For temperatures above  $T_g$ , the melt or the super cooled melt is able to reach its equilibrium state through continuous configurational changes that contribute to thermodynamic properties. These structural changes can be related to the nonArrhenian temperatures dependence of viscosity within the framework of the configurational entropy theory [7]. Studying the optical absorption, particularly the shape and shift of the absorption edge, is a very useful technique for understanding the basic mechanism of optically-induced transitions in crystalline and non-crystalline materials, as well as providing information about the energy band structure. In this paper, we report measurement of density, molar volume, Differential scanning calorimeter and Optical absorption studies of binary mixed alkali-alkaline earth oxide borate glasses.

## 2. Materials and Methods:

### Glass preparation

The oxide borate glasses of  $xK_2O-(25-x)Na_2O-12.5MgO-12.5BaO-50B_2O_3$  ( $x=0, 5, 10, 15, 20$  and  $25\text{mol}\%$ ) were prepared by the melt quenching method. The starting materials were Merck (GR grades)  $H_3BO_3$ , potassium carbonate ( $K_2CO_3$ ), Sodium oxide ( $Na_2O$ ), magnesium oxide ( $MgO$ ), barium oxide ( $BaO$ ). The calculated amounts by mol% of these compounds are thoroughly mixed and grind in Agate mortar with pestle. The ingredients were taken in to a porcelain crucible and melted in an electrically heated furnace maintained at  $1150^\circ C$  for 40 minutes. To obtain homogeneity, the melt was shaken frequently. The homogeneous melt was then quickly poured onto a stainless steel plate and pressed with another stainless steel plate, both being maintained at  $150^\circ C$ . The glass samples so obtained were subsequently annealed at  $300^\circ C$  for 6 hrs to relieve the strains. The glass samples thus obtained were clear, transparent and bubble free. All the prepared glasses are used for further experimental studies. Table -1 presents the composition of the glasses studied.

**Table 1:** Chemical Glass composition of  $xK_2O-(25-x)Na_2O-12.5MgO-12.5BaO-50B_2O_3$  glasses.

Glass System.	X (mol%)	$K_2O$ (mol%)	$Na_2O$ (mol%)	$MgO$ (mol%)	$BaO$ (mol%)	$B_2O_3$ (mol%)
NMBB1	0	0	25	12.5	12.5	50
KNMBB2	5	5	20	12.5	12.5	50
KNMBB3	10	10	15	12.5	12.5	50
KNMBB4	15	15	10	12.5	12.5	50
KNMBB5	20	20	5	12.5	12.5	50
KMBB6	25	25	0	12.5	12.5	50

**Table 2:** Physical & Optical parameters of KNMBB glasses

Physical & Optical parameters	Glass codes					
	KMBB <sub>6</sub>	KNMBB <sub>5</sub>	KNMBB <sub>4</sub>	KNMBB <sub>3</sub>	KNMBB <sub>2</sub>	NMBB <sub>1</sub>
Average molecular weight (M) (g/mol)	82.564	80.96	79.34	77.73	76.12	74.51
Density( $\rho$ ) (g/cc)	2.669	2.73	2.75	2.77	2.78	2.81
Molar Volume ( $V_M$ ) (cc/mol)	30.934	29.65	28.85	28.06	27.38	26.51
Oxygen Packing Density (g.atm/l)	64.65	67.45	69.32	71.27	73.04	75.44
Optical absorption edge (nm)	374	366	364	380	370	368
Cut-off wavelength (nm)	341	333	338	340	335	330
Direct optical band gap (eV)	3.607	3.605	3.760	3.624	3.624	3.618
Indirect optical band gap (eV)	3.343	3.459	3.369	3.360	3.369	3.407
Urbach energy $\Delta E$ (eV)	0.296	0.281	0.258	0.311	0.234	0.199
Glass transition temperature ( $T_g$ ) ( $^\circ C$ )	469	464	463	465	462	464

#### X-ray diffraction

The X-ray diffractograms were recorded at room temperature with 0.02°/sec. scanning rate in the range (10°-90°) using the Philips X-ray diffractometer with copper K $\alpha$  tube target and nickel filter operated at 40 kV, 30 mA.

#### Density and molar volume

The density ( $\rho$ ) of the glasses was determined by using the standard Archimedes's principle with xylene (99.99% pure with density 0.86 gm cm<sup>-3</sup>) as the buoyant liquid. Micro balance with sensitivity  $\pm 0.1$  mg was used for weighing the glass samples. The glass samples were suspended by a very thin copper wire. The weights of the glass samples were recorded when glass is immersed in xylene and also in air. The Oxygen Packing Density was also evaluated along with molar volume and density.

#### Differential scanning calorimetry

The thermal behaviour of the glass samples was investigated using a differential scanning calorimeter (DSC) using (Du Pont 1090). The temperature and the energy calibrations of the instrument were performed using the well-known melting temperatures and melting enthalpies of high purity tin and lead. Samples in the form of powder weighing about 15 mg were sealed in copper pans and scanned through their melting temperature with a heating rate of 10 °C/min. During all runs the sample chamber was purged with dry nitrogen.

#### Optical absorption spectra

Optical absorption spectra of all the glass samples were recorded with a (2092PIUV/VIS-Analytical Technologies Limited) UV-Vis spectrometer in the wavelength region 200 to 1000 nm. The accuracy of measured band position is  $\pm 1$  nm.

### 3. Results and Discussion:

#### X- ray diffraction

The X- ray diffraction pattern of an amorphous material is distinctly different from that of crystalline material and consists of a few broad diffuse haloes rather than sharp rings. XRD patterns of all these samples depict a diffused peak confirming the amorphous phase (vitreous state) of the glasses is shown in fig.1.

#### Density, molar volume and Glass-Transition Temperature

The density of all the glass samples was estimated from the formula

$$\rho = \left[ \frac{W_1}{(W_1 - W_2)} \times 0.86 \right] \quad (1)$$

where  $W_1$  and  $W_2$  are the weights of the glass sample in air and xylene respectively. The molar volume of glass composition was calculated using the formula,

$$V_m = \frac{\sum_i M_i}{\rho} \quad (2)$$

where  $M_i$  denotes the molar mass of the glass. The molar volume relates directly to the spatial distribution of the oxygen in the glass network. The density and molar volume values are given in Table-2. Fig.2 shows the room temperature density ( $\rho$ ) and molar volume ( $V_m$ ) variation as a function of K<sub>2</sub>O content. It is found that the density and molar volume show opposite behavior as expected and their variation with K<sub>2</sub>O content is found to be nonlinear. In general the density of glass is explained in terms of the competition between the masses and sizes of the various structural groups present. Fig.3 shows the oxygen packing density and cut-off wavelength variation as a function of K<sub>2</sub>O content it exists the oxygen packing density decreasing and cut-off wavelength varies nonlinearly with increasing of K<sub>2</sub>O content which attributed to the mixed alkali effect.

Differential scanning calorimeter (DSC) was used to characterize the glass and to determine the glass-transition temperature. Fig.4 presents the DSC thermograms of the present glass samples. The glass-transition temperature ( $T_g$ ) thermo dynamical parameter was determined and is given in Table2. Fig.5 plots the variation of the glass-transition temperature as a function of K<sub>2</sub>O content. The glass-transition temperature varies nonlinearly with K<sub>2</sub>O content indicating the presence of the MAE's influence on the thermal properties within the glass-transition region. Only recently has the structural evolution of borate glasses with temperature been

investigated. In pure  $B_2O_3$  melt, temperature induced structural changes have been described as a modification of ring statistics, with the gradual opening of the boroxol rings above the glass transition temperature ( $T_g$ ) [8–10]. In alkali borate glasses, the decrease of the number of  $BO_4$  with temperature increasing above  $T_g$  has been observed within situ high temperature [8]. A consequence of the  $BO_4$  to  $BO_3$  conversion is the formation of NBOs above  $T_g$ , which thus depolymerize the borate network and affect the melt properties.

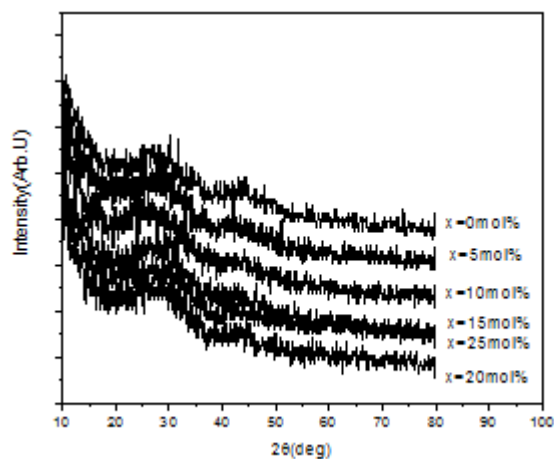


Fig 1. XRD patterns of KNMBB glasses.

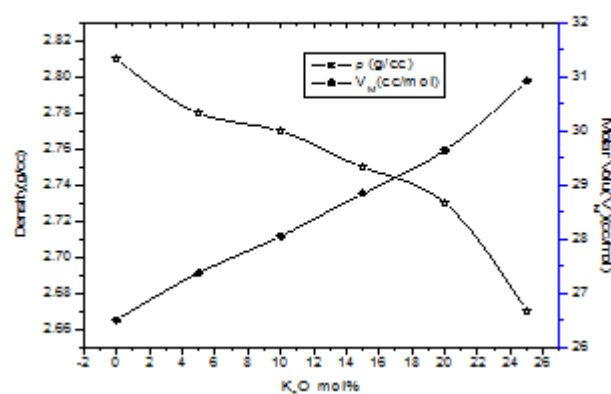


Fig 2. Variation of density and Molar volume as a function of K<sub>2</sub>O content.

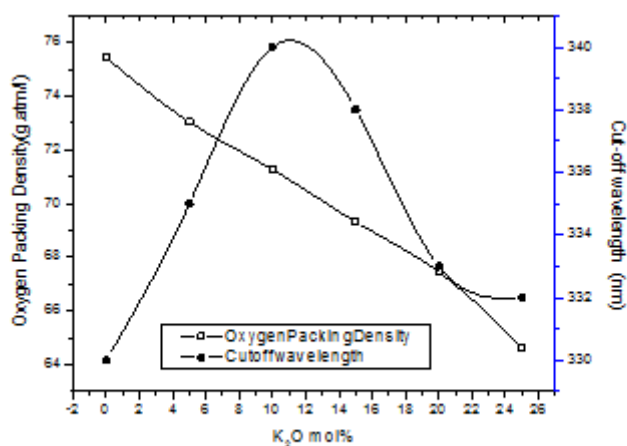


Fig 3. Variation of oxygen packing density and cut-off wavelength as a function of K<sub>2</sub>O content.

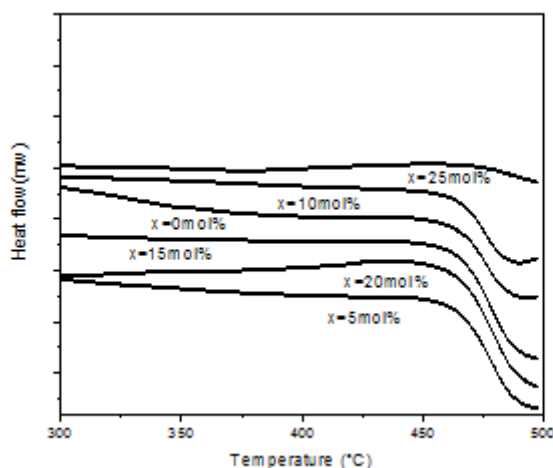


Fig 4. DSC patterns of KNMBB glasses.

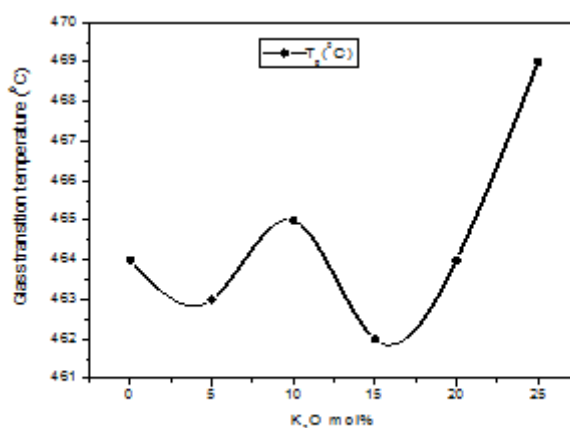


Fig 5. Variation of glass-transition temperature as a function of K<sub>2</sub>O content.

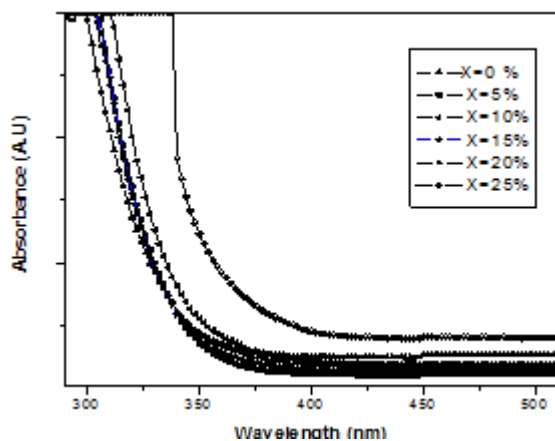


Fig 6. Optical absorption spectra of KNMBB glasses.

### Optical absorption spectra

The optical absorption spectra of  $x\text{K}_2\text{O}-(25-x)\text{Na}_2\text{O}-12.5\text{MgO}-12.5\text{BaO}-50\text{B}_2\text{O}_3$  ( $0 \leq x \leq 25$ ) glasses were recorded at room temperature and are shown in Fig.6. From the optical absorption spectra the cut-off wave length, optical edge, indirect and direct band gaps, Urbach energy values are evaluated. The optical absorption coefficient  $\alpha(\nu)$  near the fundamental absorption edge of the curve was determined from the relation:

$$\alpha(\nu) = \frac{1}{d} \log\left(\frac{I_0}{I_t}\right), \quad (3)$$

where  $I_0$  and  $I_t$  are the intensities of the incident and transmitted beams respectively, and  $d$  is the thickness of the glass sample. The factor  $\log\left(\frac{I_0}{I_t}\right)$  corresponds to the absorbance. Davis and Mott [11] and Tauc and Menth [12] related this data to the optical band gap ( $E_{opt}$ ) through the following general relation proposed for amorphous materials:

$$\alpha(\theta) = B(h\theta - E_{opt})^n/h\theta \quad (4)$$

where  $B$  is a constant and  $h\theta$  is the incident photon energy and the index  $n = 1/2$  for direct allowed transitions and  $n = 2$  for indirect transitions. From the equation (4) by plotting  $(\alpha h\theta)^2, (\alpha h\theta)^{1/2}$  as a function of photon energy  $h\theta$ , we can find the optical energy band gap  $E_{opt}$  for direct, indirect transitions. The respective values of  $E_{opt}$  were obtained by extrapolating to  $(\alpha h\theta)^{1/2} = 0$  for indirect and  $(\alpha h\theta)^2 = 0$  for direct transitions. Fig.7 and 8 shows the Tauc plots  $[(\alpha h\theta)^2, (\alpha h\theta)^{1/2}$  versus  $h\theta$ ] for the present glass samples. The optical energy band gaps for direct, indirect transitions are given in Table-2. Similar behavior was also observed by other workers [13]. The main feature of the absorption edge of amorphous materials is an exponential increase of the absorption coefficient  $\alpha(\theta)$  with the photon energy  $h\theta$ , as given by the Urbach rule [14].

$$\alpha(\theta) = C \exp\left(\frac{h\theta}{\Delta E}\right) \quad (5)$$

where  $C$  is a constant and  $\Delta E$  is the Urbach energy, which is a measure of the band shift. Fig.9. shows the variation of  $\ln(\alpha)$  as a function of photon energy  $h\theta$ . The values of the Urbach energy ( $\Delta E$ ) were determined by taking the reciprocal of the slopes of the linear portion of the  $\ln(\alpha)$  versus  $h\theta$  curves. Fig.9, illustrates a fitted curve used to determine the Urbach energy for a typical glass sample. The variation in the Urbach energy, optical band gap, cut-off wave length ( $\lambda_c$ ) and optical edge values  $\sim$  very small with  $K_2O$  content which may be due to creation of non-bridging oxygens of glass matrix. The values of the Urbach energy ( $\Delta E$ ) are presented in Table-2. The Urbach energy ( $\Delta E$ ) and  $E_{opt}$  varies nonlinearly with  $K_2O$  content as shown in Fig.10, which may be attributed to mixed alkali effect.

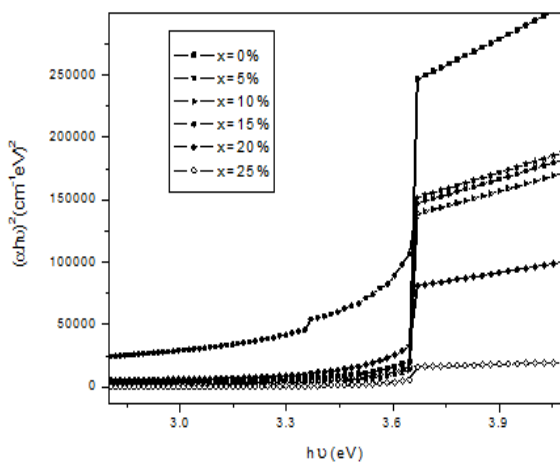


Fig 7. Taucplots  $[(\alpha h\theta)^2$  versus  $h\theta$ ] of the KNMBB glasses.

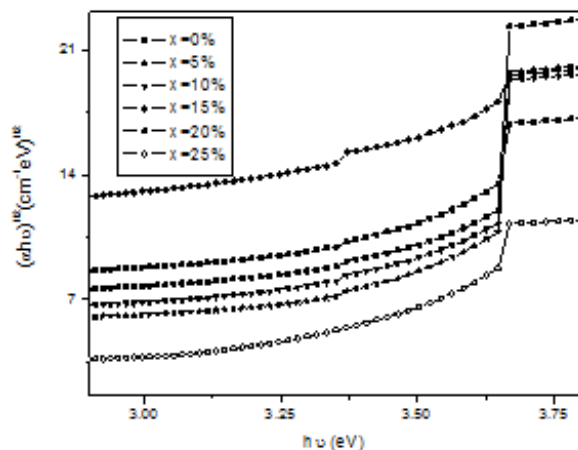


Fig 8. Tauc plots  $[(\alpha h\theta)^{1/2}$  versus  $h\theta$ ] of the KNMBB glasses.

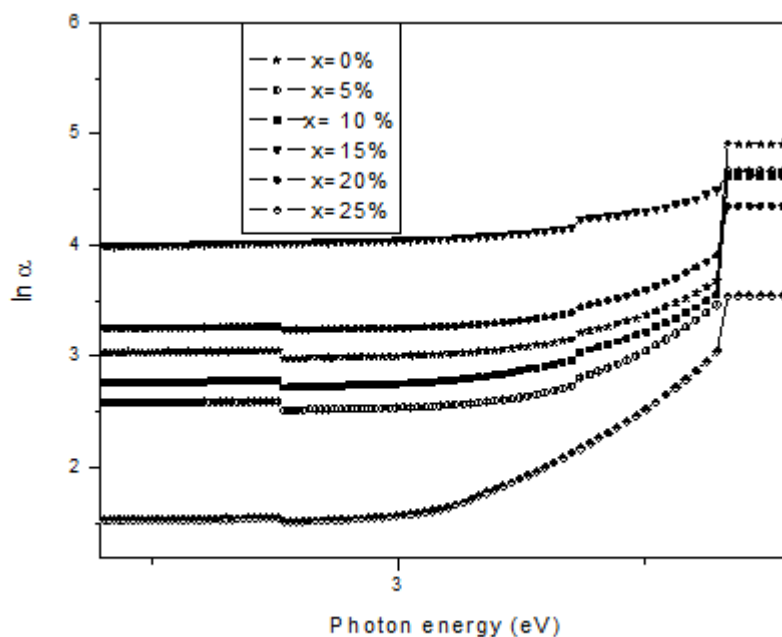


Fig 9.Urbach energy of the KNMBB glasses.

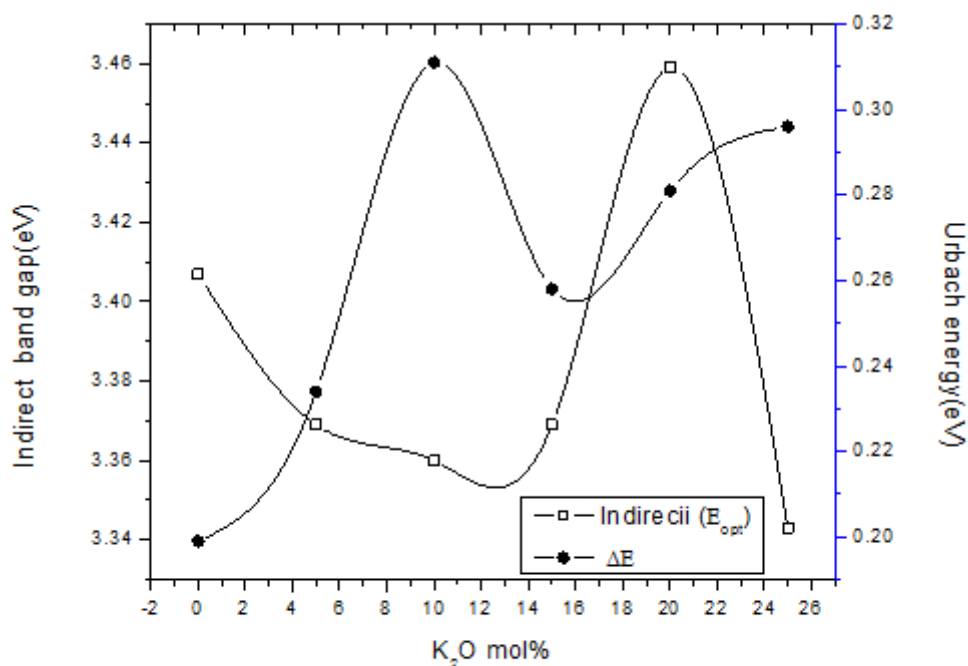


Fig 10.Variation of Indirect transition and Urbach energy as a function of K<sub>2</sub>O content.

#### 4. Conclusions:

- The absence of sharp peaks in the X-ray diffraction pattern indicated the amorphous nature of the prepared glasses.
- Density and molar volume show opposite behavior and varies nonlinearly with the K<sub>2</sub>O content which manifests the mixed alkali effect in the present glass system.
- A consequence of the BO<sub>4</sub> to BO<sub>3</sub> conversion is the formation of NBOs above T<sub>g</sub>, which thus depolymerize the borate network and affect the melt properties.

- The variation in the glass-transition temperature, Urbach energy, optical band gap, cut-off wave length ( $\lambda_c$ ), and optical edge values with K<sub>2</sub>O mol% are very small and these changes can be attributed to change in non-bridging oxygen's concentration.

**Acknowledgement:**

One of the authors, G. Srinivas, thank DST-PURSE program and UGC-New Delhi for financial assistance through RFSMS (Junior Research Fellow) program and also thanks UGC DAE CSR, Indore center and CFRD, Osmania University, Hyderabad, for providing research facilities.

**References**

- [1]. [1]. Shelby E. Introduction to Glass Science and Technology (Combridge, Royal Society of Chemistry). 1997.
- [2]. Day D E. J. Non-Cryst. Solids. 1976, 21343-72.
- [3]. Sakka S, Kamiya K and Yoshokowa H. J. Non-Cryst. Solids. 1978, 27289-93.
- [4]. Bunde A, Ingram M D and Rurs S. Phys. Chem. Chem. Phys. 2004, 63663-68.
- [5]. Imre. A W, Divinski S V, Stephan Voss, Frank Berkmeier and Helmut Mehrer. J. Non-Cryst Solids. 2006, 352783-88.
- [6]. Yiannopoulos, Y.D., Chryssikos, G.D. & Kamitsos, E.I. Structure and properties of alkaline-earth borate glasses. Phys. Chem. Glasses. 2001, 42, 164–172.
- [7]. Richet P and Neuville D. R. "Thermodynamics of Silicate Melts: Configurational Properties". pp. 132–60 in Thermodynamic Data. Systematics and Estimation, Advances in Physical Geochemistry, Edited by S. Saxena. Springer-Verlag, New York, 1992.
- [8]. Misawa M. "Structure of Vitreous and Molten B<sub>2</sub>O<sub>3</sub> Measured by Pulsed Neutron Total Scattering." J. Non-Cryst. Solids. 1990, 122, 33–40.
- [9]. Sakowski J and Herms G. "The Structure of Vitreous and Molten B<sub>2</sub>O<sub>3</sub>." J. Non-Cryst. Solids. 2001, 293–295, 304–11.
- [10]. Hassan A. K, Torell L. M, and Bo`rjesson L. "Structural Changes of B<sub>2</sub>O<sub>3</sub> through the Liquid–Glass Transition Range: A Raman-Scattering Study." Phys. Rev. B. 1992, 45, 12797–805.
- [11]. Davis E.A and Mott N.F. Phil. Mag. 22, 903, 1970.
- [12]. Tauc J. and Menth A. J. Non-Cryst. Solids. 1972, 8, 569.
- [13]. Samee M.A, Awasthi A.M, Shripathi T, Shashidhar Bale, Srinivasu Ch and Syed Rahman. "Physical and optical studies in mixed alkali borate glasses with three types of alkali ions". Journal of Alloys and Compounds. 2011, 509, 3183–3189.
- [14]. F. Urbach, Phys. Rev. 1953, 92, 1324.